© 2021. Published by The Company of Biologists Ltd | Journal of Experimental Biology (2021) 224, jeb242634. doi:10.1242/jeb.242634

RESEARCH ARTICLE

Mitochondrial K_{ATP} channels stabilize intracellular Ca^{2+} during hypoxia in retinal horizontal cells of goldfish (*Carassius auratus*)

Michael W. Country[1] and Michael G. Jonz[1,2,*]

ABSTRACT

Neurons of the retina require oxygen to survive. In hypoxia, neuronal ATP production is impaired, ATP-dependent ion pumping is reduced, transmembrane ion gradients are dysregulated, and intracellular Ca^{2+} concentration ($[Ca^{2+}]_i$) increases enough to trigger excitotoxic cell death. Central neurons of the common goldfish (*Carassius auratus*) are hypoxia tolerant, but little is known about how goldfish retinas withstand hypoxia. To study the cellular mechanisms of hypoxia tolerance, we isolated retinal interneurons (horizontal cells; HCs), and measured $[Ca^{2+}]_i$ with Fura-2. Goldfish HCs maintained $[Ca^{2+}]_i$ throughout 1 h of hypoxia, whereas $[Ca^{2+}]_i$ increased irreversibly in HCs of the hypoxia-sensitive rainbow trout (*Oncorhynchus mykiss*) with just 20 min of hypoxia. Our results suggest mitochondrial ATP-dependent K^+ channels (mK_{ATP}) are necessary to stabilize $[Ca^{2+}]_i$ throughout hypoxia. In goldfish HCs, $[Ca^{2+}]_i$ increased when mK_{ATP} channels were blocked with glibenclamide or 5-hydroxydecanoic acid, whereas the mK_{ATP} channel agonist diazoxide prevented $[Ca^{2+}]_i$ from increasing in hypoxia in trout HCs. We found that hypoxia protects against increases in $[Ca^{2+}]_i$ in goldfish HCs via mK_{ATP} channels. Glycolytic inhibition with 2-deoxyglucose increased $[Ca^{2+}]_i$, which was rescued by hypoxia in a mK_{ATP} channel-dependent manner. We found no evidence of plasmalemmal K_{ATP} channels in patch-clamp experiments. Instead, we confirmed the involvement of K_{ATP} in mitochondria with TMRE imaging, as hypoxia rapidly (<5 min) depolarized mitochondria in a mK_{ATP} channel-sensitive manner. We conclude that mK_{ATP} channels initiate a neuroprotective pathway in goldfish HCs to maintain $[Ca^{2+}]_i$ and avoid excitotoxicity in hypoxia. This model provides novel insight into the cellular mechanisms of hypoxia tolerance in the retina.

KEY WORDS: Excitotoxicity, Retina, Calcium, Mitochondria, mK_{ATP}, ATP-dependent K^+ channel

INTRODUCTION

The retina is part of the central nervous system, and therefore shares the high ATP demand of the brain (Country, 2017; Wong-Riley, 2010). Normally, over 50% of ATP supply is used to pump ions across neuronal membranes, both to maintain membrane potential and to extrude Ca^{2+} from the cytosol (Ames, 1992; Nilsson and Lutz, 2004). When neurons receive insufficient O_2 (hypoxia) or blood supply (ischemia), ATP supply is reduced, neurons depolarize, and intracellular Ca^{2+} concentration ($[Ca^{2+}]_i$) reaches toxic levels (Bickler and Buck, 1998). Several other phenomena increase $[Ca^{2+}]_i$ even further, as depolarization opens voltage-gated Ca^{2+} channels and releases excitatory neurotransmitters, such as glutamate (Szydlowska and Tymianski, 2010). High $[Ca^{2+}]_i$ is toxic to cells, and is recognized as a common final step among many pathways that trigger cell death (Bickler, 1992; Orrenius and Nicotera, 1994). This pathway from hypoxia to Ca^{2+}-mediated cell death is called excitotoxicity, and is central in strokes and several types of blindness (Bickler and Kelleher, 1992; Choi, 1992; Osborne et al., 2004).

Some species have adapted strategies to survive extended periods of hypoxia. Some turtles (e.g. *Trachemys* spp. and *Chrysemys* spp.) can survive months in hypoxic, ice-covered ponds by reducing their neuronal activity to a 'pilot light' level (Jackson and Heisler, 1982; Lutz and Nilsson, 2004). The crucian carp (*Carassius carassius*) can survive months of hypoxia at ∼4°C (Holopainen and Pitkänen, 1985; Nilsson and Lutz, 2004), and the congeneric goldfish (*Carassius auratus*) can withstand hypoxia for days at 4°C, and for hours at room temperature (Walker and Johansen, 1977; Wilkie et al., 2008). Instead of becoming quiescent during hypoxia like turtles, *Carassius* spp. maintain a reduced level of neural activity and locomotion, possibly to search out waters with greater partial pressures of O_2 (P_{O_2}) (Nilsson, 2001; Nilsson et al., 1993b; Vornanen et al., 2009; Wilkie et al., 2008). These strategies limit ATP turnover, maintain a low $[Ca^{2+}]_i$ and prevent excitotoxicity (Bickler, 1992; Bickler and Buck, 1998; Jackson, 2002; Nilsson and Lutz, 2004). The retina is also resistant to hypoxia in these species. Electroretinogram responses to light are greatly diminished during anoxia in turtle (Stensløkken et al., 2008) and carp (Johansson et al., 1997) retinas, but recover completely upon reperfusion. These studies suggest that vision withstands hypoxic insult in hypoxia-tolerant species, but the cellular mechanisms of hypoxia tolerance are completely unexplored in the retina.

Mitochondria are the major consumers of O_2 and producers of ATP, and therefore they are well positioned to sense changes in metabolite supply (Pamenter, 2014). In the turtle brain, hypoxia is sensed by mitochondrial ATP-dependent K^+ channels (mK_{ATP} channels), and the resulting mitochondrial depolarization triggers a second messenger pathway which downregulates plasma membrane ion channels and limits Ca^{2+} influx (Hawrysh and Buck, 2013; Pamenter et al., 2016; Zivkovic and Buck, 2010). mK_{ATP} channels are also required for ischemic preconditioning (IPC) in the mammalian retina, in which brief, sublethal bouts of ischemia protect against subsequent ischemic insult (Dreixler et al., 2008; Roth et al., 2006). Mitochondrial responses to hypoxia are unknown in the ectotherm retina.

Horizontal cells (HCs) are interneurons of the inner nuclear layer of the retina, which receive glutamatergic input from photoreceptors in the dark. In return, they provide inhibitory feedback to photoreceptors to improve visual contrast and colour opponency (Thoreson and Mangel, 2012; Twig et al., 2003). The Ca^{2+}-permeable ion channels, Ca^{2+} buffering mechanisms and Ca^{2+}

[1]Department of Biology, University of Ottawa, Ottawa, ON, Canada K1N 6N5. [2]Brain and Mind Research Institute, University of Ottawa, Ottawa, ON, Canada K1H 8M5.

*Author for correspondence (mjonz@uottawa.ca)

M.W.C., 0000-0001-5239-6607; M.G.J., 0000-0003-2111-1570

Received 25 March 2021; Accepted 11 August 2021

Journal of Experimental Biology (2021) 224, jeb242634. doi:10.1242/jeb.242634

pathways in HCs are well known, especially in teleost fish (reviewed in Country and Jonz, 2017). Teleost HCs present spontaneous Ca^{2+}-based action potentials (APs) both *in vitro* and *in situ* (Country et al., 2019; Country et al., 2020; Kreitzer et al., 2012; Tachibana, 1981). The function of these APs is unknown, but they have been proposed to affect feedback to photoreceptors and assist in the transition from light to dark, by rapidly depolarizing HCs (Country et al., 2019). These APs have been observed in Ca^{2+} imaging experiments (Country et al., 2019; Country et al., 2020; Kreitzer et al., 2012). Changes in APs may provide insight into how Ca^{2+} homeostasis is being maintained or threatened.

In the present study, we examined how hypoxia affects $[Ca^{2+}]_i$ in HCs. We compared responses of isolated HCs from the hypoxia-tolerant goldfish with the hypoxia-sensitive rainbow trout (*Oncorhynchus mykiss*). We showed that goldfish HCs maintained stable baseline $[Ca^{2+}]_i$ even after 1 h of hypoxia, whereas $[Ca^{2+}]_i$ increased in response to only 20 min of hypoxia in trout. We showed that hypoxia tolerance depends upon mK_{ATP} channels: blocking mK_{ATP} channels increased $[Ca^{2+}]_i$ in hypoxic goldfish HCs, whereas opening mK_{ATP} channels preserved $[Ca^{2+}]_i$ in hypoxic trout HCs. We found no evidence for K_{ATP} channel currents at the plasma membrane. Instead, we report that mitochondria depolarized in hypoxia, and that this depolarization was diminished with mK_{ATP} channel blockers. Furthermore, we present evidence that hypoxia stabilized $[Ca^{2+}]_i$ in a mK_{ATP} channel-dependent manner, preventing increases in $[Ca^{2+}]_i$ caused by blocking glycolysis. These results suggest that hypoxia triggers a neuroprotective pathway to maintain $[Ca^{2+}]_i$ homeostasis in goldfish HCs.

MATERIALS AND METHODS

Ethical approval

All animal care procedures were approved by the University of Ottawa Animal Care and Veterinary Services (protocol BL-1760), in accordance with regulations of the Canadian Council on Animal Care. Adult common goldfish, *Carassius auratus* (Linnaeus 1758) (a mix of both sexes, ranging from 7 to 60 g), were obtained from Mirdo Importations Canada (Montreal, QC, Canada), and maintained in 170 l tanks at 18°C. Rainbow trout, *Oncorhynchus mykiss* (Walbaum 1792) (a mix of both sexes, ranging from 112 to 142 g), were obtained from Linwood Acres Trout Farm (Campbellcroft, ON, Canada), and maintained in 170 l tanks at 13°C. Tanks received fresh, aerated and dechloraminated water from a constant flow-through system. Tanks were maintained on a 12 h light:12 h dark photoperiod. Fish were dark adapted for approximately 1 h, euthanized by rapid decapitation and pithed.

Isolated cell preparation

HCs were isolated according to Jonz and Barnes (2007). Unless otherwise stated, all reagents and chemicals were sourced from MilliporeSigma (Oakville, ON, Canada). Eyes were enucleated and quickly placed into ice-cold Ca^{2+}-free Ringer's solution (in mmol l^{-1}: 120 NaCl, 2.6 KCl, 10 Hepes, 0.5 NaH_2PO_4 and 16 glucose, with pH adjusted to 7.8 with NaOH). The eye was punctured at the ora serrata, and the anterior chamber of the eye was removed. The retina was carefully dissected out from the eye cup and placed in hyaluronidase (100 U ml^{-1}, cat. no. H-3506) in L-15 solution (70% Leibovitz's L-15 medium with glutamine and 30% Ca^{2+}-free Ringer's solution) at room temperature. Retinas were washed 3 times for 3 min in fresh L-15 solution, and moved to L-15 solution containing 7 U ml^{-1} papain (cat. no. 3126, Worthington Biochemical Corporation, Lakewood, NJ, USA) and 2.5 mmol l^{-1} cysteine for 40 min. Retinas were washed a further 3 times in L-15 solution, and cut into small sections (~4 mm^2). These sections were triturated 3 times to remove excess photoreceptors (Dowling et al., 1985). Then, they were moved to 1 ml of fresh L-15 solution and gently triturated to mechanically dissociate cells. The resulting cell suspension was transferred to 35 mm culture dishes (Corning Inc., Bedford, MA, USA) containing perfusion chambers (cat. no. RC-33DL, Warner Instruments Inc, Hamden, CT, USA). Dishes were pre-coated with 0.01% poly-L-lysine (cat. no. A-005-C) for 10 min, rinsed 3 times with water purified using a MilliQ system, and air-dried before use. Cells were left to settle for 15 min, and rinsed 3 times with extracellular solution (ECS; in mmol l^{-1}: 120 NaCl, 5 KCl, 2.5 $CaCl_2$, 2 $MgCl_2$, 10 Hepes and 10 glucose, with pH adjusted to 7.80 with NaOH) before dye loading.

Relative $[Ca^{2+}]_i$ measurements

Ca^{2+} imaging was performed according to Country et al. (2019). Briefly, to measure relative changes in free $[Ca^{2+}]_i$, cells were loaded with a membrane-permeant form of the Ca^{2+} indicator dye Fura-2 (Fura-2-LeakRes-AM, cat. no. 1061, Ion Biosciences, San Marcos, TX, USA). Cells were incubated with 5 µmol l^{-1} Fura-2 and 0.1% v/v of 10% w/v Pluronic F-127 (cat. no. P2443) in ECS at room temperature in the dark. After 30 min, dishes were washed 3 times with fresh ECS.

Cells were first observed with brightfield imaging using a compound microscope (FN-1, Nikon, Tokyo, Japan) and a Nikon 40× water-immersion objective (numerical aperture 0.8). HCs were identified by their characteristically large somata and thick dendrites, as in previous reports (Country et al., 2019; Dowling et al., 1985; Tachibana, 1981). For fluorescence imaging, a Lambda DG-5 wavelength changer (Sutter Instruments, Novato, CA, USA) was used to rapidly alternate between 340 and 380 nm excitation wavelengths once per second. Emission light was filtered through a 510 nm bandpass filter. Images were captured with a CCD camera (QImaging, Surrey, BC, Canada). Fluorescence ratios were recorded with NIS Elements software (Nikon), by setting circular regions of interest within HC somata. We observed no change in fluorescence ratio in cells that were not incubated in Fura-2 (n=4; not shown).

Electrophysiology

Patch-clamp recordings were taken in the whole-cell configuration. Electrodes were pulled from capillary glass (cat. no. PG52151-4, World Precision Instruments, Sarasota, FL, USA) using a vertical pipette puller (Narishige International Inc., East Meadow, NY, USA) to yield resistances of 4–8 MΩ. Electrodes were prepared immediately before recordings, and backfilled with intracellular solution (in mmol l^{-1}): 10 NaCl, 120 KCl, 2 $CaCl_2$, 2 $MgCl_2$, 5 EGTA and 10 Hepes, and adjusted to pH 7.40 with KOH. Only cells with a stable membrane seal above 1 GΩ were used. Protocols were performed with pCLAMP 7 software, an AxoPatch 1D amplifier and a DigiData 1440A digitizer (Axon Instruments, Sunnyvale, CA, USA). Signals were filtered at 5 Hz. The liquid junction potential was calculated to be 5 mV using pCLAMP 7 software and was subtracted from the pipette potential to report membrane potential.

Mitochondrial membrane potential measurements

To measure relative changes in mitochondrial membrane potential, we used tetramethylrhodamine ethyl ester (TMRE) dye (cat. no. 87917) in quenching mode. Cells were incubated at room temperature with 50 nmol l^{-1} TMRE for 30 min in the dark. Dishes were then rinsed 3 times with ECS, for 3 min per wash.

Because TMRE uptake is partially dependent upon plasma membrane potential (Perry et al., 2011), TMRE was co-applied with 100 µmol l^{-1} nifedipine in dimethyl sulfoxide (DMSO) to prevent spontaneous APs (Country et al., 2019) and to prevent subsequent loss of dye from cells. Nifedipine was maintained throughout dye loading, washes and perfusion throughout experiments.

Horizontal cells were identified in brightfield imaging as described above. For fluorescence imaging, cells were illuminated for 100 ms once every 10 s, and once per second for oligomycin and carbonyl cyanide *m*-chlorophenyl hydrazone (CCCP) controls. Excitation light was filtered through a 545 nm (±15 nm) bandpass filter; emission light was filtered through a 620 nm (±30 nm) bandpass filter. Images were captured with a CCD camera and recorded with NIS Elements software as above.

Experimental procedure and solutions

Cells were continuously superfused at ∼1 ml min^{-1} by a gravity-driven system. Solutions were drained from the recording chamber at the same rate using a peristaltic pump (Fisher Scientific, Ottawa, ON, Canada). In all imaging experiments, cells were observed for 10 min in ECS before superfusion with treatment solution. After treatment, the bath was washed with ECS for a 10 min recovery period. To create hypoxic solutions, solution reservoirs were bubbled with 100% N_2 for at least 30 min. This procedure produced recording solution with a P_{O_2} of approximately 25 mmHg (Jonz et al., 2004). Control solutions were bubbled with air for the same duration. Glibenclamide (80 µmol l^{-1}; cat. no. G0639), 5-hydroxydecanoic acid (5-HD; 100 µmol l^{-1}; cat. no. H135) and diazoxide (100 µmol l^{-1}; cat. no. D9035) were dissolved in DMSO, which never surpassed a final concentration of 0.25% v/v. At this concentration, DMSO alone had no effect on Ca^{2+} APs or Ca^{2+} baseline. To block glycolysis in experiments shown in Fig. 6, glucose was replaced with equimolar 2-deoxyglucose (2-DG; cat. no. D8375). CCCP (10 µmol l^{-1}; cat. no. 215911) and oligomycin (10 µmol l^{-1}; cat. no. 495455) were dissolved in DMSO and used as positive and negative controls, respectively, in TMRE experiments.

Analysis

For Fura-2 recordings, ratios were calculated by dividing the fluorescence emission at 340 nm by that at 380 nm following excitation at these wavelengths (F_{340}/F_{380}). These values are proportional to $[Ca^{2+}]_i$. Ratios were exported to Excel (Microsoft Corp., Redmond, WA, USA) and analysed in OriginPro 2016 (OriginLab Corp., Northampton, MA, USA). OriginPro's peak analysis gadget was used to approximate baseline using a second-derivative algorithm. The peak analysis gadget was then used to detect peaks using a local maximum function compared with baseline. For analysis, baseline was calculated as the last 30 s of baseline F_{340}/F_{380} ratio for a given time period. AP amplitude was measured as the difference between peak F_{340}/F_{380} ratio and baseline before the AP. Values of the last two APs of a given time period were averaged. For statistics, the values at the end of a treatment or recovery period were compared with the last 5 min before the treatment, and the fold-change was reported.

For TMRE imaging, fluorescence values were averaged from the last 30 s before, during and after each time period. For CCCP controls, a local maximum function was used to report peak fluorescence.

All statistical tests were performed in Prism 8 (GraphPad Software Inc., San Diego, CA, USA). Data are presented as means±s.d. In Fig. 6E,F, a Kruskal–Wallis test was used with Dunn's *post hoc* test. All columns were compared with all other columns, with a family-wise significance level of 0.05. For Fig. 8A, a one-way ANOVA was used. Holm–Šidák's *post hoc* test was used with a family-wise significance level of 0.05. All normoxic treatment groups were compared with normoxia alone, and all hypoxic groups were compared with hypoxia alone. One-tailed Mann–Whitney tests were used for all other analyses unless otherwise stated.

RESULTS

Hypoxia does not increase $[Ca^{2+}]_i$ in HCs of goldfish

HCs were isolated from goldfish and rainbow trout, and baseline $[Ca^{2+}]_i$ was monitored over time with the ratiometric Ca^{2+} imaging dye Fura-2. HCs of both species presented spontaneous Ca^{2+}-based APs for the duration of normoxic recordings as controls (Figs 1 and 2A,B). APs were similar in the two species, and matched previous reports of spontaneous, seconds- to minutes-long Ca^{2+} transients in goldfish HCs (Country et al., 2019; Kreitzer et al., 2012): APs began with a steep rise in $[Ca^{2+}]_i$ followed by a prolonged plateau and a sharp return to baseline.

To test the hypothesis that goldfish HCs (but not trout HCs) would maintain $[Ca^{2+}]_i$ baseline throughout hypoxia, we treated HCs of both species with normoxic or hypoxic solutions and monitored $[Ca^{2+}]_i$ over time. Representative brightfield images are shown in Fig. 1, along with pseudocolour representations of $[Ca^{2+}]_i$ during APs after treatment with normoxia or hypoxia. Traces of $[Ca^{2+}]_i$ over time are shown in Fig. 2A for goldfish, and Fig. 2B for trout. In goldfish HCs, $[Ca^{2+}]_i$ baseline did not change in response to 20 min normoxia (n=12) or 20 min hypoxia (n=6; Fig. 2C). Similarly, $[Ca^{2+}]_i$ did not significantly increase throughout 1 h normoxia (n=9) or 1 h hypoxia (n=5; Figs 1A–D and 2A,C).

Restoring $[Ca^{2+}]_i$ after an AP would likely require ATP for extrusion or sequestration, and APs during hypoxia may therefore strain ATP supply. We tested the hypothesis that AP amplitude would be reduced during hypoxic treatment, possibly to reduce ATP demand. Even during 1 h exposures to normoxic solution, APs persisted throughout treatment. However, in goldfish HCs, AP amplitude decreased during hypoxia (n=8; P=0.0242) when compared with normoxia (n=4; Fig. 2D). Amplitude returned to pre-treatment values upon reperfusion with normoxic solution, and there was no difference in AP amplitude between hypoxia-treated (n=7) and normoxia-treated (n=3) cells in the recovery period (Fig. 2D).

In trout HCs, $[Ca^{2+}]_i$ baseline was stable in normoxia (1.18±0.25-fold change, n=13) but increased irreversibly in response to 20 min hypoxia (1.68±0.81-fold change, n=11; Figs 1E–H and 2B,C). This represents a 50% increase in $[Ca^{2+}]_i$ compared with that in normoxia (P=0.0128). Unlike the case in goldfish HCs, AP amplitude was not significantly diminished during hypoxic treatment (normoxia n=13, hypoxia n=9; Fig. 2E). These data support the hypothesis that HCs of the hypoxia-tolerant goldfish, but not hypoxia-sensitive trout, maintain a stable $[Ca^{2+}]_i$ baseline and reduce AP amplitude during hypoxia.

mK_{ATP} channels are necessary to stabilize $[Ca^{2+}]_i$ in goldfish HCs during hypoxia

Next, we tested the hypothesis that mK_{ATP} channels might be involved in neuroprotection against hypoxia, as has been reported in turtle cortical neurons (Hogg et al., 2014; Pamenter et al., 2008b) and in IPC in the mammalian retina (Dreixler et al., 2008; Roth et al., 2006). First, we exposed isolated goldfish HCs to the mK_{ATP} channel antagonists glibenclamide (Fig. 3) and 5-HD (Fig. 4), with

Journal of Experimental Biology (2021) 224, jeb242634. doi:10.1242/jeb.242634

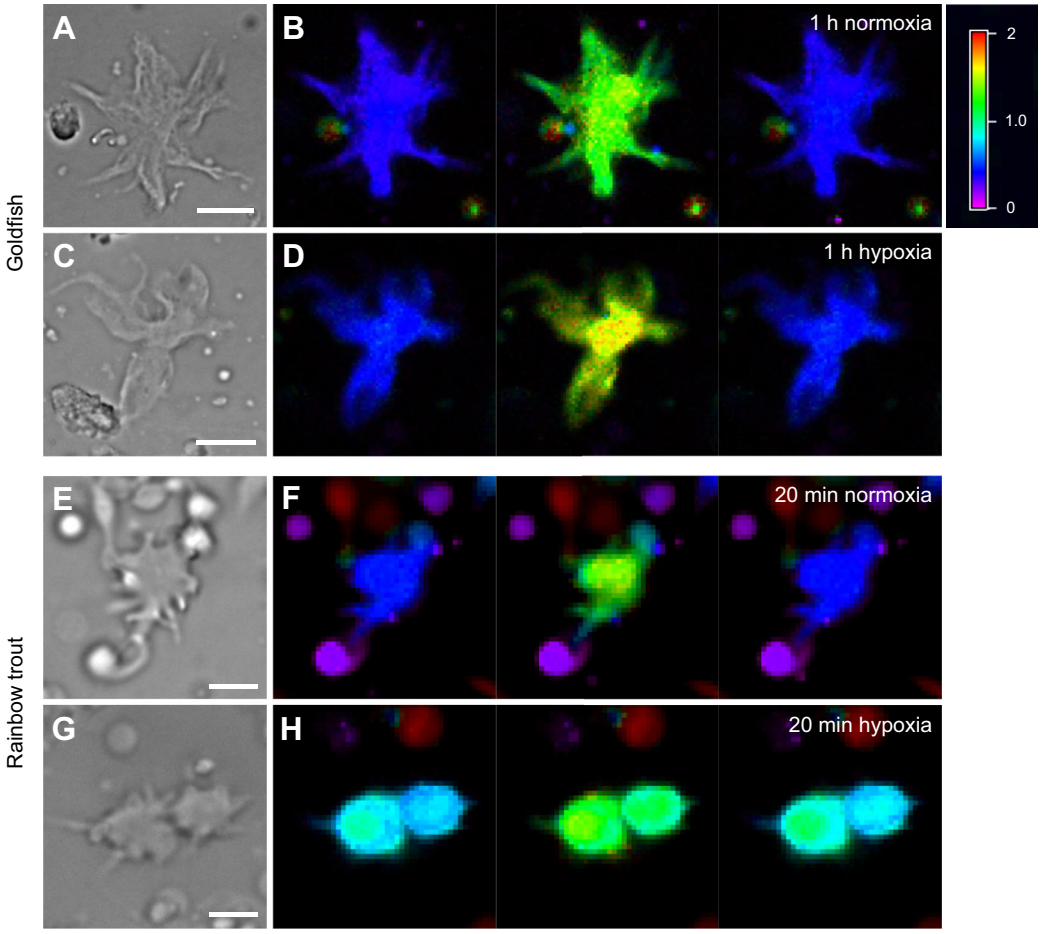

Fig. 1. Ca^{2+} imaging of action potentials in goldfish and rainbow trout horizontal cells (HCs) exposed to normoxia or hypoxia. Left, brightfield images for each cell. Right, pseudocolour fluorescence images of the Ca^{2+} indicator dye Fura-2 from which F_{340}/F_{380} ratios were calculated. Higher F_{340}/F_{380} ratios (green/yellow/red) indicate higher intracellular Ca^{2+} concentration ($[Ca^{2+}]_i$); lower ratios (blue/violet) indicate lower $[Ca^{2+}]_i$. Each triplet of fluorescence images (from left to right) represents $[Ca^{2+}]_i$ before, during and after an action potential (AP) sampled within the last 5 min of normoxia or hypoxia treatment. (A,B) Goldfish HCs maintained low $[Ca^{2+}]_i$ baseline and presented APs after superfusion with normoxic solution for 1 h. (C,D) Low $[Ca^{2+}]_i$ baseline and APs were maintained in goldfish HCs despite 1 h of hypoxia. (E,F) HCs of rainbow trout maintained the $[Ca^{2+}]_i$ baseline and APs after 20 min superfusion with normoxic solution. (G,H) 20 min of hypoxia increased the $[Ca^{2+}]_i$ baseline in trout HCs. Scale bars: 20 µm for A–D, 10 µm for E–H.

either normoxia or hypoxia for 20 min. In normoxia, glibenclamide (80 µmol l^{-1}; Pamenter et al., 2008b) had no effect on post-treatment $[Ca^{2+}]_i$ baseline (n=11; Fig. 3A). When co-applied with hypoxia, mK_{ATP} channel inhibition with glibenclamide led to an increase in $[Ca^{2+}]_i$ (1.26±0.23-fold change, n=12; Fig. 3B), a 22% increase over glibenclamide alone (P=0.0344; Fig. 3C). Consistent with the effects of hypoxia in Fig. 2D, AP amplitude decreased during treatment with glibenclamide and hypoxia (n=11) when compared with glibenclamide alone (n=10; P=0.0305; Fig. 3D). AP amplitude was partially restored when glibenclamide and hypoxia were washed out, and there was no difference in AP amplitude during recovery (normoxia n=9, hypoxia n=12; Fig. 3D).

Likewise, 20 min of 5-HD (100 µmol l^{-1}; Pamenter et al., 2008b) alone had no effect on post-treatment $[Ca^{2+}]_i$ baseline (1.00±0.07-fold change, n=8; Fig. 4A). Co-application with hypoxia increased baseline 1.06±0.08-fold (n=10; Fig. 4B). This difference was subtle (6%) but significant (P=0.0273; Fig. 4C). AP amplitude decreased slightly during application of 5-HD alone (0.81±0.23-fold change, n=6) as well as during co-application of 5-HD and hypoxia (0.84±0.15-fold change, n=9; Fig. 4D). Upon recovery, amplitude was restored and there were no differences among treatments (Fig. 4D).

mK_{ATP} channel activation is sufficient to stabilize $[Ca^{2+}]_i$ in HCs of the hypoxia-sensitive trout

To test the hypothesis that a mK_{ATP} channel-dependent pathway could stabilize $[Ca^{2+}]_i$ in trout HCs, we applied the mK_{ATP} channel agonist diazoxide (100 µmol l^{-1}; Dukoff et al., 2014; Pamenter et al., 2008b) to isolated trout HCs in the presence and absence of hypoxia. $[Ca^{2+}]_i$ baseline did not change with diazoxide alone (n=6; Fig. 5A), or when diazoxide was co-applied with hypoxia (n=10; Fig. 5B,C). AP amplitude decreased during both conditions (diazoxide and normoxia, 0.66±0.19-fold change, n=5; diazoxide and hypoxia, 0.48±0.14-fold change, n=7; Fig. 5D). The decrease in hypoxia was greater but did not differ at the prescribed level of statistical significance (P=0.053). AP amplitude increased upon reperfusion, with no differences between treatment groups (normoxia n=7, hypoxia n=8).

Hypoxia and diazoxide prevent increases in $[Ca^{2+}]_i$ baseline caused by inhibiting glycolysis

The previous experiments suggest that a mK_{ATP} channel-dependent pathway may stabilize cytosolic $[Ca^{2+}]$ baseline during hypoxia. To test whether this pathway was also active in another low-energy condition, we replaced glucose with equimolar 2-DG to block

Journal of Experimental Biology (2021) 224, jeb242634. doi:10.1242/jeb.242634

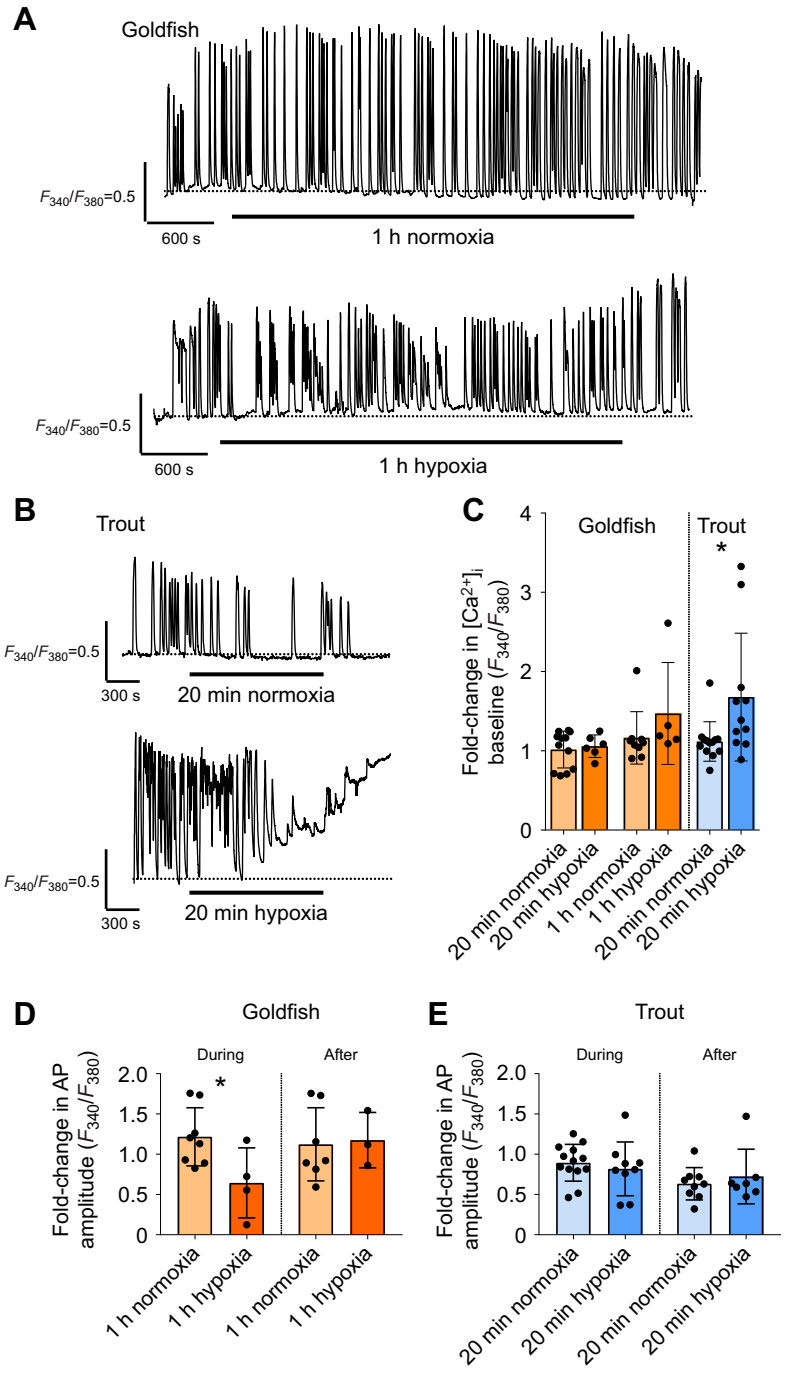

Fig. 2. Hypoxia increases $[Ca^{2+}]_i$ baseline in HCs of rainbow trout, but not goldfish. (A) Representative Fura-2-based $[Ca^{2+}]_i$ traces from goldfish HCs exposed to a normoxic solution (top) or to hypoxia (bottom) for 1 h. Ca^{2+}-based APs (represented here as transient increases in $[Ca^{2+}]_i$ throughout the traces) persisted in both conditions. The dotted horizontal line approximates an extension of the initial $[Ca^{2+}]_i$ baseline. (B) Rainbow trout HCs maintained $[Ca^{2+}]_i$ baseline and presented Ca^{2+}-based APs throughout normoxia (top). $[Ca^{2+}]_i$ baseline increased in response to 20 min hypoxia (bottom). Scale bars in A and B indicate the Fura-2 fluorescence emission ratio (F_{340}/F_{380}) and time in seconds. (C) Summary statistics of the fold-change in $[Ca^{2+}]_i$ baseline from pre-treatment values to 10 min post-treatment. $[Ca^{2+}]_i$ baseline did not increase in goldfish HCs in response to either 20 min or 1 h hypoxia. $[Ca^{2+}]_i$ increased in rainbow trout HCs after 20 min of hypoxic insult. (D,E) Fold-change in AP amplitude in goldfish HCs (D) and trout HCs (E), during and after treatment with normoxia or hypoxia. Asterisks indicate a significant difference between treatments (P<0.05).

glycolysis (Dvoriantchikova et al., 2012) in isolated goldfish HCs. Exposure to 2-DG for 1 h increased post-treatment $[Ca^{2+}]_i$, compared with 1 h normoxic controls (normoxia, 1.16±0.33-fold change, n=9; 2-DG, 2.36±1.57, n=9; P=0.0106; Fig. 6A,E). However, co-application of 2-DG and hypoxia prevented this increase almost completely (1.23±0.10-fold change, n=4; Fig. 6B,E). This protection was abolished in the presence of 5-HD (2.19±1.03-fold change, n=9; P=0.0055 versus normoxic control; Fig. 6C,E). Diazoxide (100 µmol l^{-1}), like hypoxia, prevented Ca^{2+} from increasing (1.46±0.33-fold change, n=6; Fig. 6D,E). These data further suggest a role for mK_{ATP} channels in stabilizing $[Ca^{2+}]_i$ during hypoxia in goldfish HCs.

Next, we tested whether blocking glycolysis would reduce AP amplitude, as we observed during hypoxia in previous experiments. Amplitude decreased during all treatments, when compared with normoxic controls (Fig. 6F). This decrease was significant for 2-DG (n=6; P=0.0309) and for 2-DG plus hypoxia (n=3; P=0.0219) but was not significant for 2-DG plus hypoxia and 5-HD (n=4). A decrease in amplitude was not apparent following treatment with 2-DG plus diazoxide, but because only a small proportion of cells displayed APs under these conditions, this could not be assessed. Amplitude was partially restored in all groups upon normoxic reperfusion.

No plasmalemmal K_{ATP} channel currents are detected in goldfish HCs with whole-cell patch clamp

Diazoxide, glibenclamide and 5-HD are often used to activate or block mK_{ATP} channels, but some reports suggest they may

Journal of Experimental Biology (2021) 224, jeb242634. doi:10.1242/jeb.242634

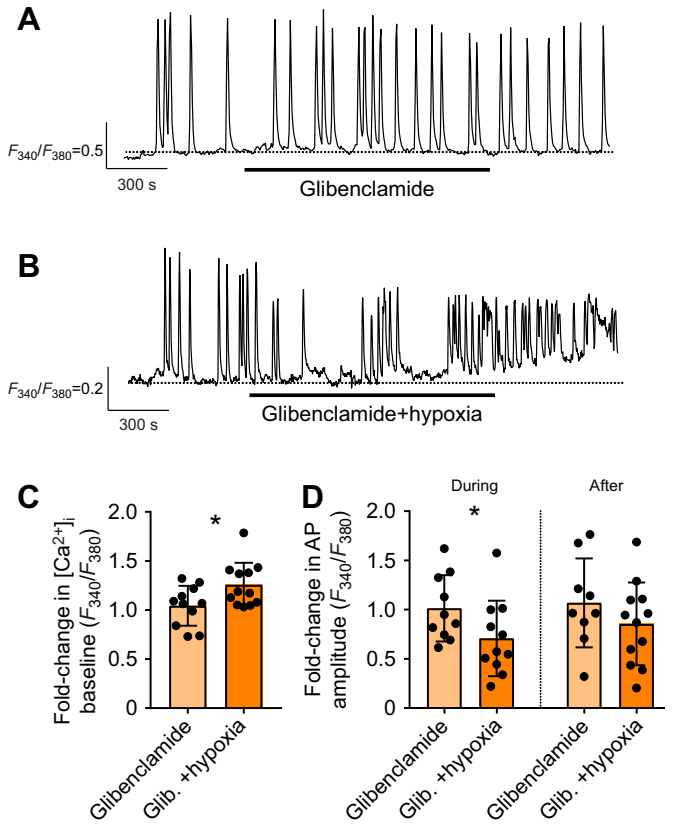

Fig. 3. Goldfish HCs do not maintain $[Ca^{2+}]_i$ in hypoxia when exposed to the mitochondrial ATP-dependent K^+ (mK_{ATP}) channel antagonist glibenclamide. (A) Representative recording of a goldfish HC exposed to 80 µmol l^{-1} glibenclamide. The dotted horizontal line is shown to illustrate that $[Ca^{2+}]_i$ baseline did not deviate throughout the 20 min exposure or during washout. (B) When co-applied with glibenclamide, hypoxia led to a subtle increase in baseline $[Ca^{2+}]_i$, as shown by the deviation from the dotted line. Scale bars in A and B indicate the Fura-2 fluorescence emission ratio (F_{340}/F_{380}) and time in seconds. The scale bar in B was expanded for clarity. (C) Summary statistics show an increase in $[Ca^{2+}]_i$ baseline. (D) Summary statistics of the fold-change in AP amplitude during and after treatment. Asterisks indicate a significant difference between treatments (P<0.05).

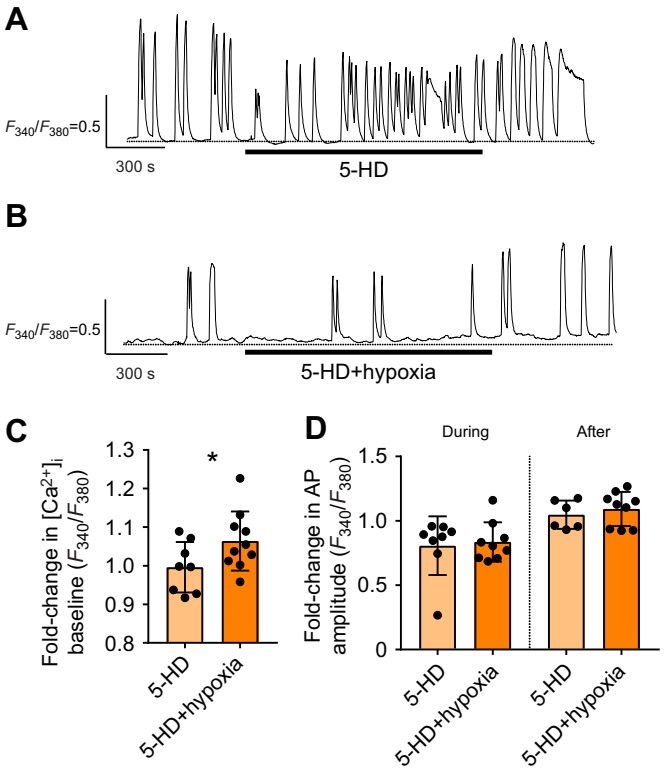

Fig. 4. Goldfish HCs do not maintain $[Ca^{2+}]_i$ in hypoxia when exposed to the mK_{ATP} channel antagonist 5-hydroxydecanoic acid (5-HD). (A) A representative trace of a goldfish HC exposed to 100 µmol l^{-1} 5-HD shows no change in $[Ca^{2+}]_i$ baseline. The dotted horizontal line is shown for clarity; baseline $[Ca^{2+}]_i$ did not deviate from this line. (B) When co-applied with 5-HD, hypoxia led to a subtle (~6%) increase in baseline $[Ca^{2+}]_i$, as shown by the deviation from the dotted line. Scale bars in A and B indicate the Fura-2 fluorescence emission ratio (F_{340}/F_{380}) and time in seconds. (C) Summary statistics show an increase in $[Ca^{2+}]_i$ baseline (P=0.0273; one-tailed Mann–Whitney). (D) Summary statistics of the fold-change in AP amplitude during and after treatment. Asterisks indicate a significant difference between treatments (P<0.05).

additionally affect K_{ATP} channels at the plasma membrane (Baumann et al., 2002; Hanley and Daut, 2005; Hill et al., 2021). HCs express at least three plasmalemmal K^+ channels (an inward rectifier, a delayed outward rectifier and a transient outward channel) (Jonz and Barnes, 2007; Lasater, 1991; Tachibana, 1983), but to our knowledge, plasmalemmal K_{ATP} channels have not been found in HCs. To test for their presence in goldfish HCs, we used whole-cell patch clamp to record membrane currents while applying the aforementioned K_{ATP} channel drugs. In the absence of these drugs, HCs presented a stable membrane current while voltage clamped to −65 mV. Hyperpolarizing and depolarizing voltage steps from −65 mV produced an 'N-shaped' profile of whole-cell currents, as in previous reports (Jonz and Barnes, 2007; Shingai and Christensen, 1986; Tachibana, 1983). Membrane currents remained stable during and after 5 min superfusion of the mK_{ATP} channel agonist diazoxide (100 µmol l^{-1}; Fig. 7A; n=5), and the I–V relationship did not change during or after treatment (Fig. 7B; n=5). Similarly, membrane currents were unchanged during and after 5 min superfusion of 5-HD (100 µmol l^{-1}; Fig. 7C,D; n=6) and glibenclamide (80 µmol l^{-1}; Fig. 7E,F; n=6).

Mitochondria depolarize early in hypoxia in a mK_{ATP} channel-dependent manner

Using TMRE imaging, we tested the hypothesis that mK_{ATP} channels open to depolarize mitochondria during hypoxia. TMRE fluorescence typically decayed gradually in normoxia (0.88±0.15-fold change within 5 min, n=23; Fig. 8A,B). Fluorescence significantly increased within 5 min of hypoxia (1.19±0.25-fold change, n=27; P<0.0001; Fig. 8A,C). Similarly, 5-HD had no significant effect alone (n=22; Fig. 8A,D), but reduced fluorescence in hypoxia by 9%. However, this effect was not significant (1.102±0.29-fold change, n=18; Fig. 8A,E). Glibenclamide alone (n=19; Fig. 8A,F) had no significant effect on fluorescence, but significantly reduced the response to hypoxia (0.99±0.15-fold change, n=14; P=0.0312; Fig. 8A,G).

At low TMRE concentrations, as mitochondria hyperpolarize, they take up more TMRE dye and fluorescence increases. But at high concentrations of TMRE, as used in the present experiments, TMRE dimerizes and quenches itself, so that fluorescence decreases as mitochondria hyperpolarize (Perry et al., 2011; Zorova et al., 2018). To confirm that TMRE attained this 'quenching mode' in our preparation, we applied CCCP, a proton ionophore, to dissipate the mitochondrial H^+ gradient and depolarize mitochondria (Brown et al., 2006; Perry et al., 2011). In quenching mode, depolarization

Journal of Experimental Biology (2021) 224, jeb242634. doi:10.1242/jeb.242634

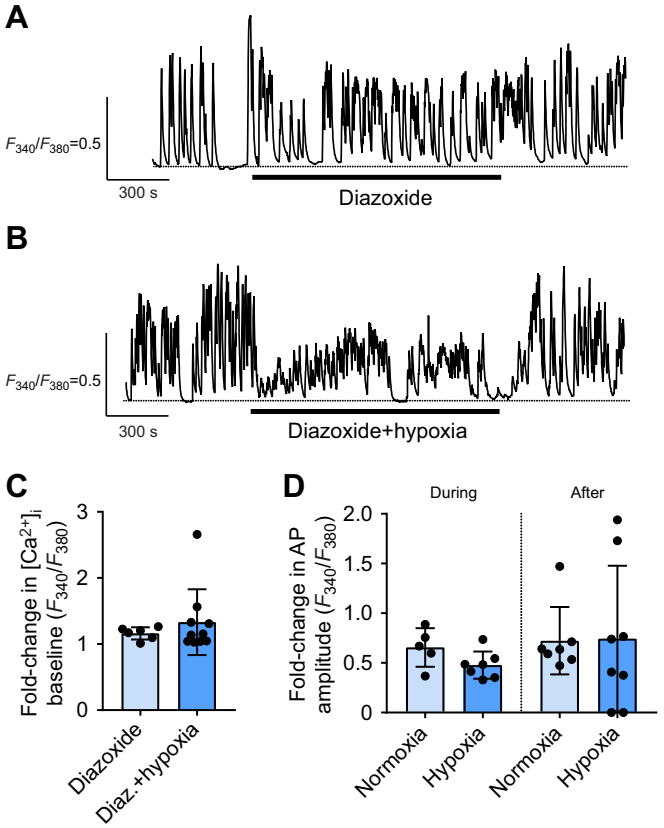

Fig. 5. Trout HCs maintain $[Ca^{2+}]_i$ baseline in hypoxia when exposed to the mK_{ATP} channel agonist diazoxide. (A) $[Ca^{2+}]_i$ baseline was unchanged in a trout HC exposed to 100 µmol l^{-1} diazoxide. The dotted horizontal line approximates an extension of initial baseline $[Ca^{2+}]_i$. (B) When co-applied with diazoxide, hypoxia did not increase $[Ca^{2+}]_i$. Amplitude decreased during the treatment and returned afterwards. Scale bars in A and B indicate the Fura-2 fluorescence emission ratio (F_{340}/F_{380}) and time in seconds. (C) Summary statistics show no increase in $[Ca^{2+}]_i$ baseline. (D) Summary statistics of the fold-change in AP amplitude during and after treatment.

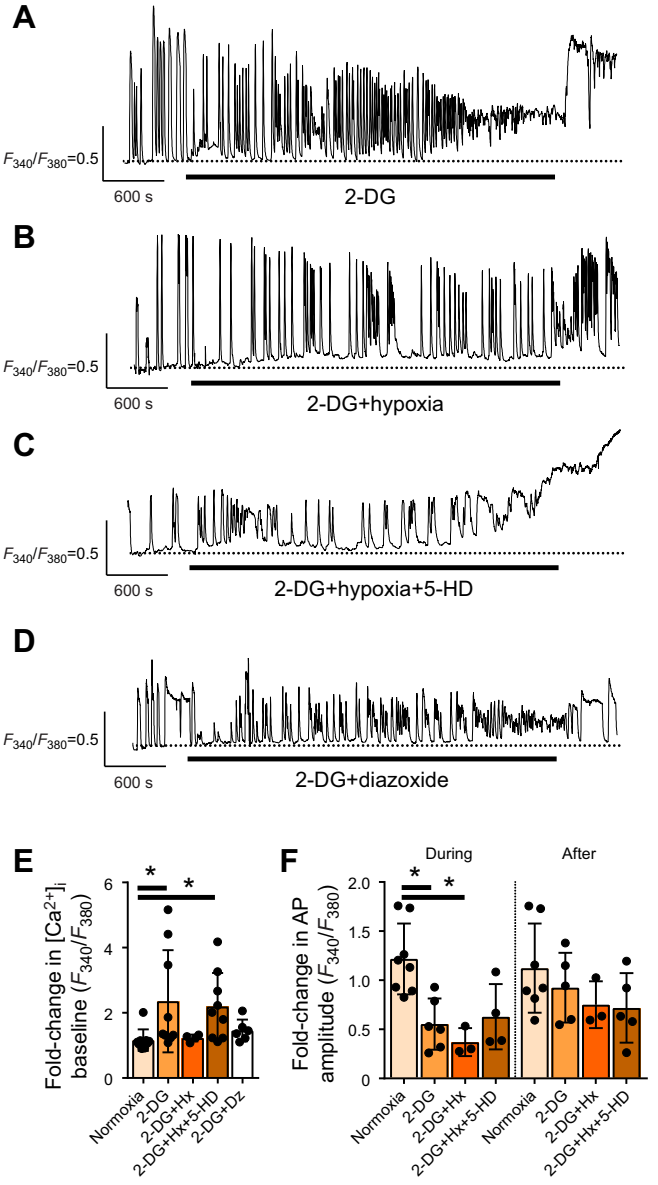

Fig. 6. Hypoxia prevents 2-deoxyglucose (2-DG)-triggered increases in $[Ca^{2+}]_i$ via a mK_{ATP} channel-dependent pathway. (A) Glycolysis was blocked by replacing glucose with equimolar (10 mmol l^{-1}) 2-DG, which led to an increase in $[Ca^{2+}]_i$. In this and subsequent panels, the dotted horizontal line approximates an extension of initial baseline $[Ca^{2+}]_i$. (B) Co-application of hypoxia prevented 2-DG from increasing $[Ca^{2+}]_i$. (C) Applying the mK_{ATP} channel antagonist 5-HD (100 µmol l^{-1}) prevented hypoxia from stabilizing $[Ca^{2+}]_i$ in the presence of 2-DG. (D) The mK_{ATP} channel agonist diazoxide (100 µmol l^{-1}) partially prevented the increase of $[Ca^{2+}]_i$ seen with 2-DG. Scale bars in A–D indicate the Fura-2 fluorescence emission ratio (F_{340}/F_{380}) and time in seconds. (E) Summary statistics show that 2-DG increased $[Ca^{2+}]_i$ compared with control (P=0.0106), as did the co-application of 2-DG with hypoxia (Hx) and 5-HD (P=0.0055; one-tailed Kruskal–Wallis with Dunn's *post hoc* test). Dz, diazoxide. (F) For AP amplitude, asterisks indicate a significant difference between treatments indicated by bars (P<0.05).

by CCCP is expected to first increase fluorescence (as dye loss reduces quenching) and then greatly diminish it (as dye concentration drops low enough to enter 'non-quenching mode') (Perry et al., 2011). In line with this model, fluorescence rapidly increased with 10 µmol l^{-1} CCCP (1.56±0.33-fold change, n=4; P<0.0001; Fig. 8A,H); then, fluorescence was nearly abolished. Oligomycin is known to block complex V of the electron transport chain, preventing the dissipation of the mitochondrial H^+ gradient and hyperpolarizing mitochondria. In our preparation, 10 µmol l^{-1} oligomycin decreased fluorescence within 5 min (0.68±0.28-fold change, n=44; P=0.0049; Fig. 8A,I).

DISCUSSION

The present study establishes part of a novel neuroprotective pathway, which maintains $[Ca^{2+}]_i$ throughout hypoxia in HCs of the hypoxia-tolerant goldfish retina. We showed that goldfish HCs require functional mK_{ATP} channels to maintain $[Ca^{2+}]_i$. Hypoxia prevented $[Ca^{2+}]_i$ from increasing in response to glycolytic inhibition with 2-DG. This protective effect was negated by the mK_{ATP} channel antagonist 5-HD and mimicked by the mK_{ATP} channel agonist diazoxide, further suggesting that mK_{ATP} channels are necessary for hypoxia tolerance. We found no evidence for plasmalemmal K_{ATP} channel currents. Instead, our data support a role for K_{ATP} channels in mitochondria, as mitochondria depolarized early in hypoxia in a mK_{ATP} channel-dependent manner.

Previous reports have shown hypoxia tolerance in the retina of *Carassius* spp. In the crucian carp, electroretinogram activity decreased during anoxia and was completely restored upon reperfusion, suggesting neuronal function and vision are not lost

Journal of Experimental Biology (2021) 224, jeb242634. doi:10.1242/jeb.242634

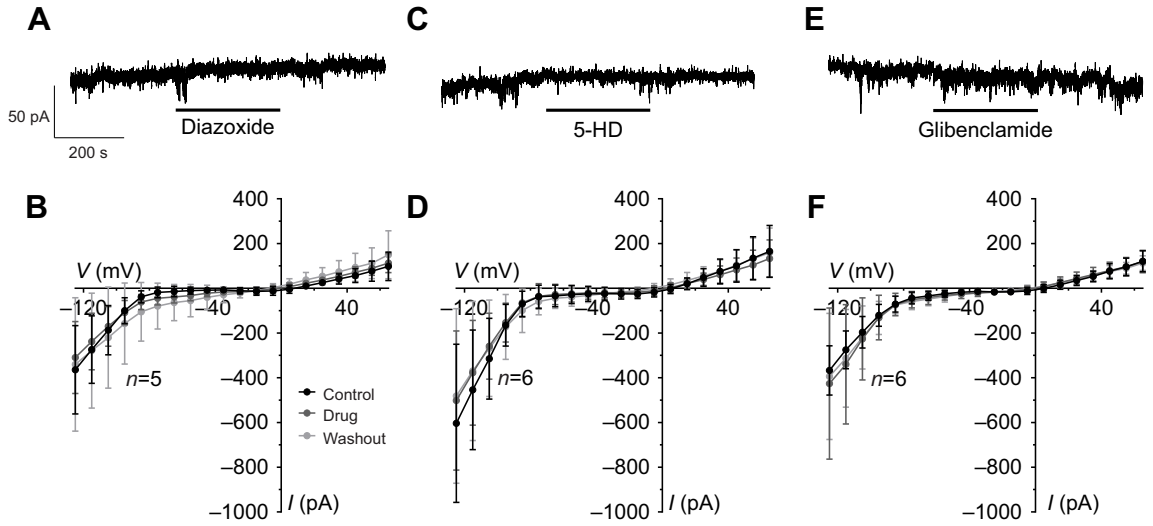

Fig. 7. mK_{ATP} channel drugs do not influence plasma membrane currents in whole-cell patch-clamp recordings of goldfish HCs. (A) Whole-cell voltage-clamp recording showed no change of plasma membrane current in response to 100 µmol l^{-1} diazoxide while held at −65 mV. (B) Current–voltage (*I–V*) relationship of 5 cells immediately before diazoxide was applied (black circles), after 5 min of perfusion with 100 µmol l^{-1} diazoxide (dark grey circles) and after 5 min of washout (light grey circles). The holding potential was −65 mV, and currents were sampled from the final 10 ms of 100 ms voltage steps. (C) 5-HD (100 µmol l^{-1}) did not affect whole-cell currents in a different HC held at −65 mV. (D) *I–V* relationship of 6 cells exposed to 5 min of 5-HD. (E) Perfusion with 80 µmol l^{-1} glibenclamide did not affect whole-cell currents in a HC held at −65 mV. (F) *I–V* curves for 6 cells exposed to 5 min of glibenclamide. Scale bar in A (for A, C and E) represents whole-cell current (pA) and time in seconds.

by anoxic insult (Johansson et al., 1997). In the goldfish retina, metabotropic glutamate receptors protected against apoptosis caused by 3 h of hypoxia and reperfusion at room temperature (Beraudi et al., 2007). In the present study, we showed that neurons of the goldfish retina resisted hypoxic increases in $[Ca^{2+}]_i$, which have been established as a precursor to excitotoxic cell death (Choi, 1992; Szydlowska and Tymianski, 2010).

The present study demonstrated that a mK_{ATP} channel-dependent pathway is required to stabilize $[Ca^{2+}]_i$ baseline in goldfish HCs. This work agrees with a growing body of evidence which shows a central role for mK_{ATP} channels and mitochondria in protection against hypoxia across a wide array of tissues and species. mK_{ATP} channel protection has been shown in diverse organs in mammals including the heart (O'Rourke, 2004; Obal et al., 2005; Wang et al., 2001), brain (Heurteaux et al., 1995), kidney (O'Sullivan et al., 2008; Rahgozar et al., 2003), liver (O'Sullivan et al., 2008) and retina (Dreixler et al., 2008; Ettaiche et al., 2001; Roth et al., 2006). Likewise, mK_{ATP} channels protect against hypoxia in hypoxia-tolerant species, including in the turtle brain (Dukoff et al., 2014; Pamenter et al., 2008b) and in cardiomyocytes of hypoxia-tolerant fish, such as the goldfish (Chen et al., 2005), the yellowtail flounder (*Limanda ferruginea*) (MacCormack and Driedzic, 2002) and the armoured catfish (*Liposarcus pardalis*) (MacCormack et al., 2003).

Among hypoxia-tolerant species, the neuronal mechanisms of hypoxia tolerance have been best studied in cortical neurons of the red-eared slider turtle (*Trachemys scripta*). These neurons maintained $[Ca^{2+}]_i$ for hours in hypoxia, but not when glycolysis was inhibited with iodoacetate (Bickler, 1992). Pre-treating brain slices with anoxia protected against iodoacetate insult, similar to how hypoxia prevented increases in $[Ca^{2+}]_i$ during glycolytic inhibition in the present study. Furthermore, mK_{ATP} channels were necessary for neuroprotection in painted turtle (*Chrysemys picta*) cortical neurons (Pamenter et al., 2008b; Zivkovic and Buck, 2010), and may have conferred neuroprotection in HCs in the present report.

Although the exact mechanisms of mK_{ATP} channel-dependent neuroprotection in turtles have yet to be established, there is evidence that hypoxia opens mK_{ATP} channels, which depolarizes mitochondria, triggering a subtle release of Ca^{2+} via the mitochondrial permeability transition pore (Hawrysh and Buck, 2013; Pamenter et al., 2008b; Zivkovic and Buck, 2010). This slight increase in $[Ca^{2+}]_i$ activates second messenger pathways and ultimately downregulates AMPA receptors (Pamenter et al., 2008a; Zivkovic and Buck, 2010), NMDA receptors (Pamenter et al., 2008b; Shin et al., 2005), and Ca^{2+}-dependent K^+ (K_{Ca}) channels (Rodgers-Garlick et al., 2013). This downregulation of membrane currents, or 'channel arrest' (Hochachka, 1986), would limit Ca^{2+} influx and reduce the ATP required to maintain transmembrane ion gradients, so as to conserve energy during hypoxia. Channel arrest has been demonstrated in the goldfish brain (Wilkie et al., 2008), but not yet in the goldfish retina.

The mK_{ATP} channel protection we observed likely involves a different pathway from that of the turtle brain. In contrast with the turtle model, we did not observe an immediate increase in $[Ca^{2+}]_i$ after applying hypoxia to goldfish HCs, suggesting any mK_{ATP} channel pathway in goldfish HCs is Ca^{2+} independent. Instead, we report that mK_{ATP} channel blockade increased $[Ca^{2+}]_i$ in hypoxia, whereas in the turtle, mK_{ATP} channel activation increased $[Ca^{2+}]_i$ (Hawrysh and Buck, 2013; Pamenter et al., 2008b). Mitochondrial Ca^{2+} release may not be a feasible strategy in HCs because they appear to have few mitochondria. Mitochondria are scarce in electron micrographs (Dowling and Boycott, 1966; Yamada and Ishikawa, 1965) and cytochrome *c* oxidase labelling is weak in HC somata (Kageyama and Meyer, 1988). Furthermore, Ca^{2+} is elevated in darkness, so a Ca^{2+}-dependent pathway might not be feasible (Country and Jonz, 2017; Hayashida and Yagi, 2002).

Our results may align more closely with IPC in the mammalian retina, which is also Ca^{2+} independent. In the rat retina, mK_{ATP} channels are both necessary and sufficient for IPC (Dreixler et al., 2008; Roth et al., 2006; Stokfisz et al., 2017). Once open, mK_{ATP} activates two Ca^{2+}-independent isoforms of protein kinase C (PKC): PKC-δ and PKC-ε (Dreixler et al., 2008). HCs likely benefit because IPC prevents thinning of the inner nuclear and outer

Journal of Experimental Biology (2021) 224, jeb242634. doi:10.1242/jeb.242634

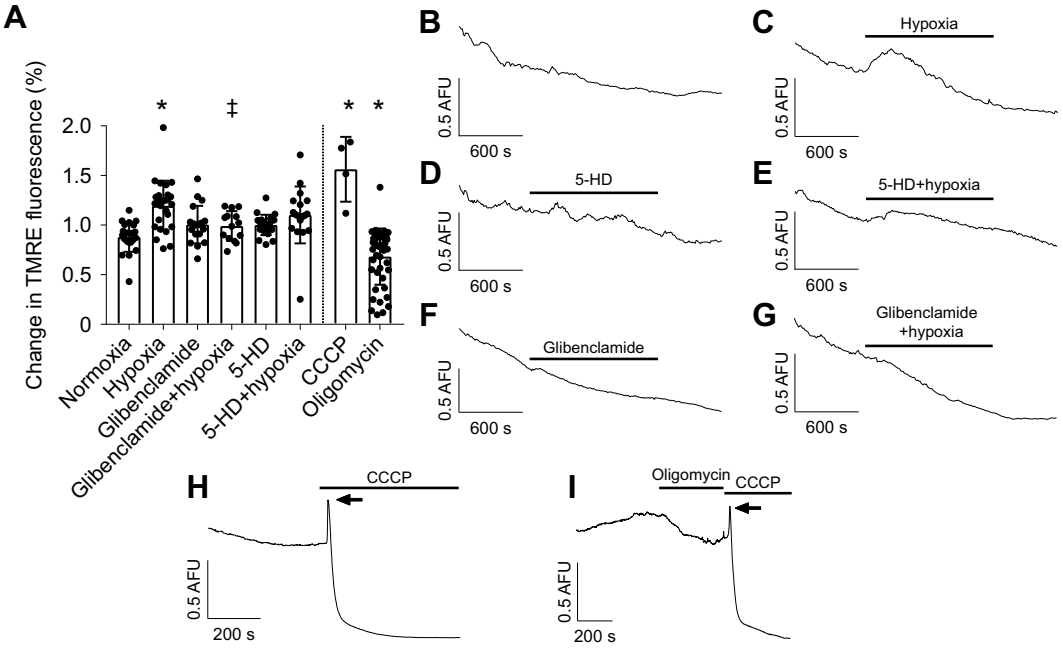

Fig. 8. Mitochondria in goldfish HCs depolarize early in hypoxia as a result of mK_{ATP} channel activity. (A) TMRE fluorescence was measured before and 5 min after various treatments, and the percentage change is reported here. Symbols indicate significance as compared with normoxic (*) and hypoxic (‡) groups. (B–G) TMRE fluorescence in response to the following treatments: B, normoxia; C, hypoxia; D, 100 µmol l^{-1} 5-HD; E, 5-HD+hypoxia; F, 80 µmol l^{-1} glibenclamide; and G, glibenclamide+hypoxia. CCCP (10 µmol l^{-1}; H) and oligomycin (10 µmol l^{-1}; I) were used as positive and negative controls, respectively, to confirm the dye was in its 'quenching' mode (so that mitochondrial depolarizations produced increased fluorescence). CCCP is known to lead to a rapid increase (arrows) and then a decrease in fluorescence as the dye concentration drops low enough to enter non-quenching mode (see Results). Therefore, in A, CCCP data represent the percentage change from pre-application to peak fluorescence. Scale bars in B–I represent relative changes in fluorescence (in arbitrary fluorescence units, AFU) and time in seconds.

plexiform layers (Roth et al., 1998; Toprak et al., 2002; Zhu et al., 2007), and the δ isoform localizes to mammalian HCs (Dreixler et al., 2008). It is possible that neuroprotection is Ca^{2+} independent in both mammalian and goldfish HCs, because $[Ca^{2+}]_i$ is already elevated throughout darkness as a result of constant glutamatergic input from photoreceptors. Future experiments could compare this HC pathway with neuroprotection in the inner retina (e.g. ganglion cells), as inner retinal neurons are not expected to undergo prolonged increases in $[Ca^{2+}]_i$ during the dark, unlike HCs.

These models may offer insight into how mK_{ATP} channels open in the goldfish retina. Local decreases in [ATP] have been proposed to increase mK_{ATP} channel open probability in the turtle (Hogg et al., 2014), yet this is unlikely in goldfish HCs because blocking glycolysis dysregulated $[Ca^{2+}]_i$ in the current study. Adenosine and A1/A2a receptors are necessary for neuroprotection in the turtle (Buck and Bickler, 1995; Pérez-Pinzón et al., 1993) and they open mK_{ATP} channels during IPC in the mammalian retina (Li and Roth, 1999; Li et al., 2000). Adenosine may be a likely candidate as adenylates are released by goldfish HCs, where they may buffer the synaptic cleft pH and modulate feedback to cones (Vroman et al., 2014). Other candidate mK_{ATP} channel openers include nitric oxide and mitochondrion-specific isoforms of PKC (Korge et al., 2002; Sasaki et al., 2000). PKC is present in HCs of the catfish (Pfeiffer-Linn and Lasater, 1998) and nitric oxide synthase is present in goldfish H1 cells (Daniels and Baldridge, 2011).

The specificity of mK_{ATP} channel agonists and antagonists has been called into question, as has the existence of mK_{ATP} channels (reviewed in Garlid and Halestrap, 2012; Roth et al., 2006). Glibenclamide may inhibit plasmalemmal K_{ATP} channels, and 5-HD is a fatty acid which can interfere with lipid oxidation in mitochondria (Hanley and Daut, 2005). Although diazoxide is over 1000 times more specific for mK_{ATP} channels than for plasmalemmal K_{ATP} channels (Garlid et al., 1996), it has been shown to inhibit complex II of the electron transport chain and to lead to mitochondrial uncoupling (Kowaltowski et al., 2001). However, these off-target effects may require higher concentrations than those used in mK_{ATP} channel experiments (Garlid and Halestrap, 2012; Kowaltowski et al., 2001), and they are not themselves sufficient to explain the drugs' neuroprotective impacts in hypoxia (reviewed in O'Rourke, 2004; Roth et al., 2006). The present report provides further evidence for mK_{ATP} channels, as we show mitochondrial depolarization was dependent on K_{ATP} channels yet we found no evidence for K_{ATP} channel currents at the plasma membrane. Perhaps most convincingly, mK_{ATP} channel proteins were recently reconstituted and shown to confer protection via IPC and activation by diazoxide (Paggio et al., 2019), supporting the existence and protective role of mK_{ATP} channels. They are expressed and mediate hypoxic protection in a wide range of species, including *Caenorhabditis elegans* (Wojtovich et al., 2012), turtles (Dukoff et al., 2014; Pamenter et al., 2008b), rats (Piriou et al., 2000; Roth et al., 2006) and humans (Jiang et al., 2006). In fish, mK_{ATP} channels have been found in the goldfish heart (Chen et al., 2005) and trout liver (Onukwufor et al., 2016).

In the present study, AP amplitude was reduced as ATP supply was challenged with hypoxia or with inhibition of glycolysis. Reductions in AP amplitude may be a neuroprotective response to hypoxia, so as to limit Ca^{2+} influx and reduce the ATP demand for extrusion via Ca^{2+} ATPases. In support of this theory, mK_{ATP} channel activation in trout reduced AP amplitude and stabilized $[Ca^{2+}]_i$ baseline. However, reductions in AP amplitude were not sufficient to maintain $[Ca^{2+}]_i$, as $[Ca^{2+}]_i$ was dysregulated

in multiple conditions despite amplitude reductions (i.e. glibenclamide and hypoxia; 2-DG; 2-DG, hypoxia and 5-HD). This may be an example of channel arrest, either of L-type Ca^{2+} channels or of ryanodine receptors (Country et al., 2019), to limit increases in $[Ca^{2+}]_i$ during APs. Channel arrest is known to protect neurons of the goldfish telencephalon (Wilkie et al., 2008) and the turtle cortex (Pamenter et al., 2008a,b; Rodgers-Garlick et al., 2013); however, to our knowledge it has yet to be shown in the retina.

Rainbow trout have been shown to be sensitive to hypoxia in previous reports (e.g. Hylland et al., 1995; Iftikar et al., 2010; Nilsson et al., 1993a), and a-, b-, and c-waves of the trout electroretinogram were all negatively affected by hypoxia (Ubels, 1979). Our results confirmed the hypoxia sensitivity of trout retinal neurons. Furthermore, activating mK_{ATP} channels in trout HCs prevented hypoxia from increasing $[Ca^{2+}]_i$ baseline, suggesting the mechanisms of hypoxia tolerance downstream of mK_{ATP} channel activation are conserved among fish. An additional take-home point from these studies relates to the hypoxia sensitivity of HCs, more generally. In mammals, HCs were resistant to excitotoxic cell death (Kim et al., 2010), possibly because they have adapted to long periods of high $[Ca^{2+}]_i$ in the dark. By showing that $[Ca^{2+}]_i$ is dysregulated in trout but not goldfish, our results suggest that neuroprotection is specific to goldfish, and not to HCs more generally. Furthermore, we showed that trout HCs are susceptible to hypoxic cell death even in the absence of glutamate. But in the dark, glutamate from photoreceptors increases HC Ca^{2+} to a steady concentration of ∼600 nmol l^{-1} (Hayashida and Yagi, 2002), so that more ATP turnover would be required to maintain Ca^{2+} homeostasis. The mK_{ATP} channel pathway and other forms of neuroprotection are likely even more crucial for cell survival in darkness.

Turtles are often considered the champions of hypoxia tolerance, partly because they greatly reduce electrical activity in their brains during anoxia, compared with modest reductions in goldfish and crucian carp (Nilsson and Lutz, 2004). But in the retina, this paradigm may be reversed. Electroretinogram recordings suggest electrical activity in the turtle retina is reduced modestly (50%) in hypoxia (Stensløkken et al., 2008), and turtles respond to visual stimuli during their hibernation (Madsen et al., 2013). Carp shows upwards of a 90% reduction in electroretinogram activity in hypoxia (Johansson et al., 1997). Given this difference, the *Carassius* retina merits consideration as a novel model of neuroprotection against hypoxia. This model may be important because strokes, and the majority of retinal diseases of the eye, involve ischaemic cell death (Hayreh and Zimmerman, 2005; Osborne et al., 2004). Blood flow is negatively affected in the eye in branch and central retinal artery occlusions, retinal vein occlusions and glaucoma (Hayreh and Zimmerman, 2005; Osborne et al., 2004, 1999). Other diseases, such as age-related macular degeneration and diabetic retinopathy, can leave affected areas of the retina hypoxic, leading to cell death and vision loss (Blasiak et al., 2014; Sim et al., 2014). By clarifying the cellular mechanisms by which goldfish retinal neurons survive hypoxia, we may learn of new strategies to mitigate or prevent retinal disease and protect vision.

Conclusion

The present study revealed a novel mK_{ATP} channel-dependent mechanism which may protect the vertebrate retina from hypoxia. We showed that $[Ca^{2+}]_i$ was dysregulated in hypoxia in HCs of the hypoxia-sensitive trout; in contrast, HCs of the hypoxia-tolerant goldfish maintained $[Ca^{2+}]_i$ even after 1 h of hypoxia. mK_{ATP} channels were necessary to stabilize $[Ca^{2+}]_i$ in goldfish HCs and sufficient for Ca^{2+} homeostasis in trout HCs. We ruled out the involvement of plasmalemmal K_{ATP} channels, while showing that mK_{ATP} channels depolarize mitochondria early in hypoxia. Finally, we showed that hypoxia stabilized $[Ca^{2+}]_i$ even as glycolysis was inhibited. This novel *in vitro* model is the first to explore intrinsic hypoxia tolerance in retinal neurons, and may lead to novel insights to protect against ischaemic diseases of the eye.

Acknowledgements

The authors thank Benjamin F. N. Campbell for advice, and Dr Kathleen M. Gilmour for generously providing rainbow trout.

Competing interests

The authors declare no competing or financial interests.

Author contributions

Conceptualization: M.W.C., M.G.J.; Methodology: M.W.C., M.G.J.; Validation: M.W.C., M.G.J.; Formal analysis: M.W.C.; Investigation: M.W.C., M.G.J.; Resources: M.G.J.; Data curation: M.W.C.; Writing - original draft: M.W.C.; Writing - review & editing: M.G.J.; Supervision: M.G.J.; Project administration: M.G.J.; Funding acquisition: M.G.J.

Funding

This research was supported by Natural Sciences and Engineering Research Council of Canada (NSERC) grants (no. 342303 and 05571) to M.G.J., and M.W.C. was funded in part by Queen Elizabeth II Graduate Scholarship for Science and Technology (QEII-GSST), and Natural Sciences and Engineering Research Council of Canada post-graduate scholarships.

References

Ames, A. (1992). Energy requirements of CNS cells as related to their function and to their vulnerability to ischemia: a commentary based on studies on retina. *Can. J. Physiol. Pharmacol.* **70**, S158-S164. doi:10.1139/y92-257

Baumann, P., Poitry, S., Roatti, A. and Baertschi, A. J. (2002). Plasmalemmal K_{ATP} channels shape triggered calcium transients in metabolically impaired rat atrial myocytes. *Am. J. Physiol. Heart Circ. Physiol.* **283**, H2296-H2305. doi:10.1152/ajpheart.00393.2002

Beraudi, A., Bruno, V., Battaglia, G., Biagioni, F., Rampello, L., Nicoletti, F. and Poli, A. (2007). Pharmacological activation of mGlu2/3 metabotropic glutamate receptors protects retinal neurons against anoxic damage in the goldfish *Carassius auratus*. *Exp. Eye Res.* **84**, 544-552. doi:10.1016/j.exer.2006.11.008

Bickler, P. E. (1992). Cerebral anoxia tolerance in turtles: regulation of intracellular calcium and pH. *Am. J. Physiol.* **263**, R1298-R1302. doi:10.1152/ajpregu.1992.263.6.R1298

Bickler, P. E. and Buck, L. T. (1998). Adaptations of vertebrate neurons to hypoxia and anoxia: maintaining critical Ca^{2+} concentrations. *J. Exp. Biol.* **201**, 1141-1152. doi:10.1242/jeb.201.8.1141

Bickler, P. E. and Kelleher, J. A. (1992). Fructose-1,6-bisphosphate stabilizes brain intracellular calcium during hypoxia in rats. *Stroke* **23**, 1617-1622. doi:10.1161/01.STR.23.11.1617

Blasiak, J., Petrovski, G., Veréb, Z., Facskó, A. and Kaarniranta, K. (2014). Oxidative stress, hypoxia, and autophagy in the neovascular processes of age-related macular degeneration. *Biomed. Res. Int.* **2014**, 768026. doi:10.1155/2014/768026

Brown, M. R., Sullivan, P. G. and Geddes, J. W. (2006). Synaptic mitochondria are more susceptible to Ca^{2+} overload than nonsynaptic mitochondria. *J. Biol. Chem.* **281**, 11658-11668. doi:10.1074/jbc.M510303200

Buck, L. T. and Bickler, P. E. (1995). Role of adenosine in NMDA receptor modulation in the cerebral cortex of an anoxia-tolerant turtle (*Chrysemys picta belli*). *J. Exp. Biol.* **198**, 1621-1628. doi:10.1242/jeb.198.7.1621

Chen, J., Zhu, J. X., Wilson, I. and Cameron, J. S. (2005). Cardioprotective effects of KATP channel activation during hypoxia in goldfish Carassius auratus. *J. Exp. Biol.* **208**, 2765-2772. doi:10.1242/jeb.01704

Choi, D. W. (1992). Excitotoxic cell death. *J. Neurobiol.* **23**, 1261-1276. doi:10.1002/neu.480230915

Country, M. W. (2017). Retinal metabolism: a comparative look at energetics in the retina. *Brain Res.* **1672**, 50-57. doi:10.1016/j.brainres.2017.07.025

Country, M. W. and Jonz, M. G. (2017). Calcium dynamics and regulation in horizontal cells of the vertebrate retina: lessons from teleosts. *J. Neurophysiol.* **117**, 523-536. doi:10.1152/jn.00585.2016

Country, M. W., Campbell, B. F. N. and Jonz, M. G. (2019). Spontaneous action potentials in retinal horizontal cells of goldfish (Carassius auratus) are dependent upon L-type Ca(2+) channels and ryanodine receptors. *J. Neurophysiol.* **122**, 2284-2293. doi:10.1152/jn.00240.2019

Country, M. W., Htite, E. D., Samson, I. A. and Jonz, M. G. (2020). Retinal horizontal cells of goldfish (Carassius auratus) display subtype-specific differences in spontaneous action potentials in situ. *J. Comp. Neurol.* **529**, 1756-1767. doi:10.1002/cne.25054

Daniels, B. A. and Baldridge, W. H. (2011). The light-induced reduction of horizontal cell receptive field size in the goldfish retina involves nitric oxide. *Vis. Neurosci.* **28**, 137-144. doi:10.1017/S0952523810000490

Dowling, J. E. and Boycott, B. B. (1966). Organization of the primate retina: electron microscopy. *Proc. R. Soc. Lond. B Biol. Sci.* **166**, 80-111. doi:10.1098/rspb.1966.0086

Dowling, J. E., Pak, M. W. and Lasater, E. M. (1985). White perch horizontal cells in culture: methods, morphology and process growth. *Brain Res.* **360**, 331-338. doi:10.1016/0006-8993(85)91250-8

Dreixler, J. C., Shaikh, A. R., Shenoy, S. K., Shen, Y. and Roth, S. (2008). Protein kinase C subtypes and retinal ischemic preconditioning. *Exp. Eye Res.* **87**, 300-311. doi:10.1016/j.exer.2008.05.015

Dukoff, D. J., Hogg, D. W., Hawrysh, P. J. and Buck, L. T. (2014). Scavenging ROS dramatically increase NMDA receptor whole-cell currents in painted turtle cortical neurons. *J. Exp. Biol.* **217**, 3346-3355. doi:10.1242/jeb.105825

Dvoriantchikova, G., Ivanov, D., Barakat, D., Grinberg, A., Wen, R., Slepak, V. Z. and Shestopalov, V. I. (2012). Genetic ablation of Pannexin1 protects retinal neurons from ischemic injury. *PLoS ONE* **7**, e31991. doi:10.1371/journal.pone.0031991

Ettaiche, M., Heurteaux, C., Blondeau, N., Borsotto, M., Tinel, N. and Lazdunski, M. (2001). ATP-sensitive potassium channels (K(ATP)) in retina: a key role for delayed ischemic tolerance. *Brain Res.* **890**, 118-129. doi:10.1016/S0006-8993(00)03152-8

Garlid, K. D. and Halestrap, A. P. (2012). The mitochondrial K(ATP) channel–fact or fiction? *J. Mol. Cell. Cardiol.* **52**, 578-583. doi:10.1016/j.yjmcc.2011.12.011

Garlid, K. D., Paucek, P., Yarov-Yarovoy, V., Sun, X. and Schindler, P. A. (1996). The mitochondrial K_{ATP} channel as a receptor for potassium channel openers. *J. Biol. Chem.* **271**, 8796-8799. doi:10.1074/jbc.271.15.8796

Hanley, P. J. and Daut, J. (2005). K(ATP) channels and preconditioning: a re-examination of the role of mitochondrial K(ATP) channels and an overview of alternative mechanisms. *J. Mol. Cell. Cardiol.* **39**, 17-50. doi:10.1016/j.yjmcc.2005.04.002

Hawrysh, P. J. and Buck, L. T. (2013). Anoxia-mediated calcium release through the mitochondrial permeability transition pore silences NMDA receptor currents in turtle neurons. *J. Exp. Biol.* **216**, 4375-4387. doi:10.1242/jeb.092650

Hayashida, Y. and Yagi, T. (2002). On the interaction between voltage-gated conductances and Ca^{2+} regulation mechanisms in retinal horizontal cells. *J. Neurophysiol.* **87**, 172-182. doi:10.1152/jn.00778.2000

Hayreh, S. S. and Zimmerman, M. B. (2005). Central retinal artery occlusion: visual outcome. *Am. J. Ophthalmol.* **140**, 376-391. doi:10.1016/j.ajo.2005.03.038

Heurteaux, C., Lauritzen, I., Widmann, C. and Lazdunski, M. (1995). Essential role of adenosine, adenosine A1 receptors, and ATP-sensitive K^+ channels in cerebral ischemic preconditioning. *Proc. Natl. Acad. Sci. USA* **92**, 4666-4670. doi:10.1073/pnas.92.10.4666

Hill, E., Gowers, R., Richardson, M. J. E. and Wall, M. J. (2021). α-synuclein aggregates increase the conductance of substantia nigra dopamine neurons, an effect partly reversed by the K_{ATP} channel inhibitor glibenclamide. *eneuro* **8**, ENEURO.0330-20. doi:10.1523/ENEURO.0330-20.2020

Hochachka, P. W. (1986). Defense strategies against hypoxia and hypothermia. *Science* **231**, 234-241. doi:10.1126/science.2417316

Hogg, D. W., Hawrysh, P. J. and Buck, L. T. (2014). Environmental remodelling of GABAergic and glutamatergic neurotransmission: rise of the anoxia-tolerant turtle brain. *J. Therm. Biol.* **44**, 85-92. doi:10.1016/j.jtherbio.2014.01.003

Holopainen, I. J. and Pitkänen, A. K. (1985). Population size and structure of crucian carp (Carassius carassius (L.)) in two small, natural ponds in Eastern Finland. *Annales Zoologici Fennici* 22, 397-406.

Hylland, P., Nilsson, G. E. and Johansson, D. (1995). Anoxic brain failure in an ectothermic vertebrate: release of amino acids and K^+ in rainbow trout thalamus. *Am. J. Physiol.* **269**, R1077-R1084. doi:10.1152/ajpregu.1995.269.5.R1077

Iftikar, F. I., Matey, V. and Wood, C. M. (2010). The ionoregulatory responses to hypoxia in the freshwater rainbow trout *Oncorhynchus mykiss*. *Physiol. Biochem. Zool.* **83**, 343-355. doi:10.1086/648566

Jackson, D. C. (2002). Hibernating without oxygen: physiological adaptations of the painted turtle. *J. Physiol.* **543**, 731-737. doi:10.1113/jphysiol.2002.024729

Jackson, D. C. and Heisler, N. (1982). Plasma ion balance of submerged anoxic turtles at 3°C: The role of calcium lactate formation. *Respir. Physiol.* **49**, 159-174. doi:10.1016/0034-5687(82)90071-8

Jiang, M. T., Ljubkovic, M., Nakae, Y., Shi, Y., Kwok, W.-M., Stowe, D. F. and Bosnjak, Z. J. (2006). Characterization of human cardiac mitochondrial ATP-sensitive potassium channel and its regulation by phorbol ester in vitro. *Am. J. Physiol. Heart Circ. Physiol.* **290**, H1770-H1776. doi:10.1152/ajpheart.01084.2005

Johansson, D., Nilsson, G. E. and Døving, K. B. (1997). Anoxic depression of light-evoked potentials in retina and optic tectum of crucian carp. *Neurosci. Lett.* **237**, 73-76. doi:10.1016/S0304-3940(97)00814-8

Jonz, M. G. and Barnes, S. (2007). Proton modulation of ion channels in isolated horizontal cells of the goldfish retina. *J. Physiol.* **581**, 529-541. doi:10.1113/jphysiol.2006.125666

Jonz, M. G., Fearon, I. M. and Nurse, C. A. (2004). Neuroepithelial oxygen chemoreceptors of the zebrafish gill. *J. Physiol.* **560**, 737-752. doi:10.1113/jphysiol.2004.069294

Kageyama, G. H. and Meyer, R. L. (1988). Histochemical localization of cytochrome oxidase in the retina and optic tectum of normal goldfish: a combined cytochrome oxidase-horseradish peroxidase study. *J. Comp. Neurol.* **270**, 354-371. doi:10.1002/cne.902700305

Kim, S. A., Jeon, J. H., Son, M. J., Cha, J., Chun, M.-H. and Kim, I.-B. (2010). Changes in transcript and protein levels of calbindin D28k, calretinin and parvalbumin, and numbers of neuronal populations expressing these proteins in an ischemia model of rat retina. *Anat. Cell Biol.* **43**, 218-229. doi:10.5115/acb.2010.43.3.218

Korge, P., Honda, H. M. and Weiss, J. N. (2002). Protection of cardiac mitochondria by diazoxide and protein kinase C: implications for ischemic preconditioning. *Proc. Natl. Acad. Sci. USA* **99**, 3312-3317. doi:10.1073/pnas.052713199

Kowaltowski, A. J., Seetharaman, S., Paucek, P. and Garlid, K. D. (2001). Bioenergetic consequences of opening the ATP-sensitive K^+ channel of heart mitochondria. *Am. J. Physiol. Heart Circ. Physiol.* **280**, H649-H657. doi:10.1152/ajpheart.2001.280.2.H649

Kreitzer, M. A., Jacoby, J., Naylor, E., Baker, A., Grable, T., Tran, E., Booth, S. E., Qian, H. and Malchow, R. P. (2012). Distinctive patterns of alterations in proton efflux from goldfish retinal horizontal cells monitored with self-referencing H^+-selective electrodes. *Eur. J. Neurosci.* **36**, 3040-3050. doi:10.1111/j.1460-9568.2012.08226.x

Lasater, E. M. (1991). Membrane properties of distal retinal neurons. *Prog. Retin. Res.* **11**, 215-246. doi:10.1016/0278-4327(91)90030-6

Li, B. and Roth, S. (1999). Retinal ischemic preconditioning in the rat: requirement for adenosine and repetitive induction. *Invest. Ophthalmol. Vis. Sci.* **40**, 1200-1216.

Li, B., Yang, C., Rosenbaum, D. M. and Roth, S. (2000). Signal transduction mechanisms involved in ischemic preconditioning in the rat retina in vivo. *Exp. Eye Res.* **70**, 755-765. doi:10.1006/exer.2000.0843

Lutz, P. L. and Nilsson, G. E. (2004). Vertebrate brains at the pilot light. *Respir. Physiol. Neurobiol.* **141**, 285-296. doi:10.1016/j.resp.2004.03.013

MacCormack, T. J. and Driedzic, W. R. (2002). Mitochondrial ATP-sensitive K^+ channels influence force development and anoxic contractility in a flatfish, yellowtail flounder *Limanda ferruginea*, but not Atlantic cod *Gadus morhua* heart. *J. Exp. Biol.* **205**, 1411-1418. doi:10.1242/jeb.205.10.1411

MacCormack, T. J., Treberg, J. R., Almeida-Val, V. M. F., Val, A. L. and Driedzic, W. R. (2003). Mitochondrial KATP channels and sarcoplasmic reticulum influence cardiac force development under anoxia in the Amazonian armored catfish Liposarcus pardalis. *Comp. Biochem. Physiol. A Mol. Integr. Physiol.* **134**, 441-448. doi:10.1016/S1095-6433(02)00315-X

Madsen, J. G., Wang, T., Beedholm, K. and Madsen, P. T. (2013). Detecting spring after a long winter: coma or slow vigilance in cold, hypoxic turtles? *Biol. Lett.* **9**, 20130602.

Nilsson, G. E. (2001). Surviving anoxia with the brain turned on. *News Physiol. Sci.* **16**, 217-221. doi:10.1152/physiologyonline.2001.16.5.217

Nilsson, G. E. and Lutz, P. L. (2004). Anoxia tolerant brains. *J. Cereb. Blood Flow Metab.* **24**, 475-486. doi:10.1097/00004647-200405000-00001

Nilsson, G. E., Pérez-Pinzón, M., Dimberg, K. and Winberg, S. (1993a). Brain sensitivity to anoxia in fish as reflected by changes in extracellular K+ activity. *Am. J. Physiol. Regul. Integr. Comp. Physiol.* **264**, R250-R253. doi:10.1152/ajpregu.1993.264.2.R250

Nilsson, G. E., Rosen, P. R. and Johansson, D. (1993b). Anoxic depression of spontaneous locomotor-activity in crucian carp quantified by a computerized imaging technique. *J. Exp. Biol.* **180**, 153-162. doi:10.1242/jeb.180.1.153

Obal, D., Dettwiler, S., Favoccia, C., Scharbatke, H., Preckel, B. and Schlack, W. (2005). The influence of mitochondrial K_{ATP}-channels in the cardioprotection of preconditioning and postconditioning by sevoflurane in the rat in vivo. *Anesth. Analg.* **101**, 1252-1260. doi:10.1213/01.ANE.0000181336.96511.32

Onukwufor, J. O., Stevens, D. and Kamunde, C. (2016). Bioenergetic and volume regulatory effects of mitoK_{ATP} channel modulators protect against hypoxia-reoxygenation-induced mitochondrial dysfunction. *J. Exp. Biol.* **219**, 2743-2751.

O'Rourke, B. (2004). Evidence for mitochondrial K^+ channels and their role in cardioprotection. *Circ. Res.* **94**, 420-432. doi:10.1161/01.RES.0000117583.66950.43

Orrenius, S. and Nicotera, P. (1994). The calcium ion and cell death. *J. Neural. Transm. Suppl.* **43**, 1-11.

Osborne, N. N., Ugarte, M., Chao, M., Chidlow, G., Bae, J. H., Wood, J. P. M. and Nash, M. S. (1999). Neuroprotection in relation to retinal ischemia and relevance to glaucoma. *Surv. Ophthalmol.* **43** Suppl. 1, S102-S128. doi:10.1016/S0039-6257(99)00044-2

Osborne, N. N., Casson, R. J., Wood, J. P. M., Chidlow, G., Graham, M. and Melena, J. (2004). Retinal ischemia: mechanisms of damage and potential

therapeutic strategies. *Prog. Retin. Eye Res.* **23**, 91-147. doi:10.1016/j.preteyeres.2003.12.001

O'Sullivan, J. C., Fu, D., Alam, H. B. and McCabe, J. T. (2008). Diazoxide increases liver and kidney HSP25 and HSP70 after shock and stroke. *J. Surg. Res.* **149**, 120-130. doi:10.1016/j.jss.2007.12.750

Paggio, A., Checchetto, V., Campo, A., Menabò, R., Di Marco, G., Di Lisa, F., Szabo, I., Rizzuto, R. and De Stefani, D. (2019). Identification of an ATP-sensitive potassium channel in mitochondria. *Nature* **572**, 609-613. doi:10.1038/s41586-019-1498-3

Pamenter, M. E. (2014). Mitochondria: a multimodal hub of hypoxia tolerance. *Can. J. Zool.* **92**, 569-589. doi:10.1139/cjz-2013-0247

Pamenter, M. E., Shin, D. S.-H. and Buck, L. T. (2008a). AMPA receptors undergo channel arrest in the anoxic turtle cortex. *Am. J. Physiol. Regul. Integr. Comp. Physiol.* **294**, R606-R613. doi:10.1152/ajpregu.00433.2007

Pamenter, M. E., Shin, D. S.-H., Cooray, M. and Buck, L. T. (2008b). Mitochondrial ATP-sensitive K^+ channels regulate NMDAR activity in the cortex of the anoxic western painted turtle. *J. Physiol.* **586**, 1043-1058. doi:10.1113/jphysiol.2007.142380

Pamenter, M. E., Gomez, C. R., Richards, J. G. and Milsom, W. K. (2016). Mitochondrial responses to prolonged anoxia in brain of red-eared slider turtles. *Biol. Lett.* **12**, 20150797. doi:10.1098/rsbl.2015.0797

Pérez-Pinzón, M. A., Lutz, P. L., Sick, T. J. and Rosenthal, M. (1993). Adenosine, a "retaliatory" metabolite, promotes anoxia tolerance in turtle brain. *J. Cereb. Blood Flow Metab.* **13**, 728-732. doi:10.1038/jcbfm.1993.93

Perry, S. W., Norman, J. P., Barbieri, J., Brown, E. B. and Gelbard, H. A. (2011). Mitochondrial membrane potential probes and the proton gradient: a practical usage guide. *BioTechniques* **50**, 98-115. doi:10.2144/000113610

Pfeiffer-Linn, C. L. and Lasater, E. M. (1998). Multiple second-messenger system modulation of voltage-activated calcium currents in teleost retinal horizontal cells. *J. Neurophysiol.* **80**, 377-388. doi:10.1152/jn.1998.80.1.377

Piriou, V., Chiari, P., Knezynski, S., Bastien, O., Loufoua, J., Lehot, J.-J., Foëx, P., Annat, G. and Ovize, M. (2000). Prevention of isoflurane-induced preconditioning by 5-hydroxydecanoate and gadolinium: possible involvement of mitochondrial adenosine triphosphate-sensitive potassium and stretch-activated channels. *Anesthesiology* **93**, 756-764. doi:10.1097/00000542-200009000-00025

Rahgozar, M., Willgoss, D. A., Gobé, G. C. and Endre, Z. H. (2003). ATP-dependent K^+ channels in renal ischemia reperfusion injury. *Ren. Fail.* **25**, 885-896. doi:10.1081/JDI-120026024

Rodgers-Garlick, C. I., Hogg, D. W. and Buck, L. T. (2013). Oxygen-sensitive reduction in Ca^{2+}-activated K^+ channel open probability in turtle cerebrocortex. *Neuroscience* **237**, 243-254. doi:10.1016/j.neuroscience.2013.01.046

Roth, S., Li, B., Rosenbaum, P. S., Gupta, H., Goldstein, I. M., Maxwell, K. M. and Gidday, J. M. (1998). Preconditioning provides complete protection against retinal ischemic injury in rats. *Invest. Ophthalmol. Vis. Sci.* **39**, 777-785.

Roth, S., Dreixler, J. C., Shaikh, A. R., Lee, K. H. and Bindokas, V. (2006). Mitochondrial potassium ATP channels and retinal ischemic preconditioning. *Invest. Ophthalmol. Vis. Sci.* **47**, 2114-2124. doi:10.1167/iovs.05-1068

Sasaki, N., Sato, T., Ohler, A., O'Rourke, B. and Marbán, E. (2000). Activation of mitochondrial ATP-dependent potassium channels by nitric oxide. *Circulation* **101**, 439-445. doi:10.1161/01.CIR.101.4.439

Shin, D. S.-H., Wilkie, M. P., Pamenter, M. E. and Buck, L. T. (2005). Calcium and protein phosphatase 1/2A attenuate *N*-methyl-D-aspartate receptor activity in the anoxic turtle cortex. *Comp. Biochem. Physiol. A Mol. Integr. Physiol.* **142**, 50-57. doi:10.1016/j.cbpa.2005.07.017

Shingai, R. and Christensen, B. N. (1986). Excitable properties and voltage-sensitive ion conductances of horizontal cells isolated from catfish (*Ictalurus punctatus*) retina. *J. Neurophysiol.* **56**, 32-49. doi:10.1152/jn.1986.56.1.32

Sim, D. A., Keane, P. A., Rajendram, R., Karampelas, M., Selvam, S., Powner, M. B., Fruttiger, M., Tufail, A. and Egan, C. A. (2014). Patterns of peripheral retinal and central macula ischemia in diabetic retinopathy as evaluated by ultra-widefield fluorescein angiography. *Am. J. Ophthalmol.* **158**, 144-153.e1. doi:10.1016/j.ajo.2014.03.009

Stensløkken, K.-O., Milton, S. L., Lutz, P. L., Sundin, L., Renshaw, G. M. C., Stecyk, J. A. W. and Nilsson, G. E. (2008). Effect of anoxia on the electroretinogram of three anoxia-tolerant vertebrates. *Comp. Biochem. Physiol. A Mol. Integr. Physiol.* **150**, 395-403. doi:10.1016/j.cbpa.2008.03.022

Stokfisz, K., Ledakowicz-Polak, A., Zagorski, M. and Zielinska, M. (2017). Ischaemic preconditioning - Current knowledge and potential future applications after 30 years of experience. *Adv. Med. Sci.* **62**, 307-316. doi:10.1016/j.advms.2016.11.006

Szydlowska, K. and Tymianski, M. (2010). Calcium, ischemia and excitotoxicity. *Cell Calcium* **47**, 122-129. doi:10.1016/j.ceca.2010.01.003

Tachibana, M. (1981). Membrane properties of solitary horizontal cells isolated from goldfish retina. *J. Physiol.* **321**, 141-161. doi:10.1113/jphysiol.1981.sp013976

Tachibana, M. (1983). Ionic currents of solitary horizontal cells isolated from goldfish retina. *J. Physiol.* **345**, 329-351. doi:10.1113/jphysiol.1983.sp014981

Thoreson, W. B. and Mangel, S. C. (2012). Lateral interactions in the outer retina. *Prog. Retin. Eye Res.* **31**, 407-441. doi:10.1016/j.preteyeres.2012.04.003

Toprak, A. B., Ozbilgin, K., Toprak, V., Tuglu, I. and Guler, C. (2002). A histological analysis of the protective effect of ischemic preconditioning in the rat retina. *Curr. Eye Res.* **24**, 234-239. doi:10.1076/ceyr.24.3.234.8308

Twig, G., Levy, H. and Perlman, I. (2003). Color opponency in horizontal cells of the vertebrate retina. *Prog. Retin. Eye Res.* **22**, 31-68. doi:10.1016/S1350-9462(02)00045-9

Ubels, J. L. (1979). Retinomotor activity and the c-wave of the hypoxic trout retina. *Invest. Ophthalmol. Vis. Sci.* **18**, 756-761.

Vornanen, M., Stecyk, J. A. W. and Nilsson, G. E. (2009). The anoxia-tolerant Crucian carp (*Carassius carassius L.*). *Fish Physiol.* **27**, 397-441. doi:10.1016/S1546-5098(08)00009-5

Vroman, R., Klaassen, L. J., Howlett, M. H. C., Cenedese, V., Klooster, J., Sjoerdsma, T. and Kamermans, M. (2014). Extracellular ATP hydrolysis inhibits synaptic transmission by increasing pH buffering in the synaptic cleft. *PLoS Biol.* **12**, e1001864. doi:10.1371/journal.pbio.1001864

Walker, R. M. and Johansen, P. H. (1977). Anaerobic metabolism in goldfish (*Carassius auratus*). *Can. J. Zool.* **55**, 1304-1311. doi:10.1139/z77-170

Wang, S., Cone, J. and Liu, Y. (2001). Dual roles of mitochondrial K(ATP) channels in diazoxide-mediated protection in isolated rabbit hearts. *Am. J. Physiol. Heart Circ. Physiol.* **280**, H246-H255. doi:10.1152/ajpheart.2001.280.1.H246

Wilkie, M. P., Pamenter, M. E., Alkabie, S., Carapic, D., Shin, D. S. H. and Buck, L. T. (2008). Evidence of anoxia-induced channel arrest in the brain of the goldfish (*Carassius auratus*). *Comp. Biochem. Physiol. C Toxicol. Pharmacol.* **148**, 355-362. doi:10.1016/j.cbpc.2008.06.004

Wojtovich, A. P., DiStefano, P., Sherman, T., Brookes, P. S. and Nehrke, K. (2012). Mitochondrial ATP-sensitive potassium channel activity and hypoxic preconditioning are independent of an inwardly rectifying potassium channel subunit in *Caenorhabditis elegans*. *FEBS Lett.* **586**, 428-434. doi:10.1016/j.febslet.2012.01.021

Wong-Riley, M. T. (2010). Energy metabolism of the visual system. *Eye Brain* **2**, 99-116. doi:10.2147/EB.S9078

Yamada, E. and Ishikawa, T. (1965). The fine structure of the horizontal cells in some vertebrate retinae. *Cold Spring Harb. Symp. Quant. Biol.* **30**, 383-392. doi:10.1101/SQB.1965.030.01.038

Zhu, Y., Zhang, Y., Ojwang, B. A., Brantley, M. A., , Jr and Gidday, J. M. (2007). Long-term tolerance to retinal ischemia by repetitive hypoxic preconditioning: role of HIF-1α and heme oxygenase-1. *Invest. Ophthalmol. Vis. Sci.* **48**, 1735-1743. doi:10.1167/iovs.06-1037

Zivkovic, G. and Buck, L. T. (2010). Regulation of AMPA receptor currents by mitochondrial ATP-sensitive K^+ channels in anoxic turtle neurons. *J. Neurophysiol.* **104**, 1913-1922. doi:10.1152/jn.00506.2010

Zorova, L. D., Popkov, V. A., Plotnikov, E. Y., Silachev, D. N., Pevzner, I. B., Jankauskas, S. S., Babenko, V. A., Zorov, S. D., Balakireva, A. V., Juhaszova, M. et al. (2018). Mitochondrial membrane potential. *Anal. Biochem.* **552**, 50-59. doi:10.1016/j.ab.2017.07.009